

U

LEVEL II

①

SECURITY CLASSIFICATION OF THIS PAGE (When Data Entered)

REPORT DOCUMENTATION PAGE		READ INSTRUCTIONS BEFORE COMPLETING FORM
1. REPORT NUMBER	2. GOVT ACCESSION NO.	3. RECIPIENT'S CATALOG NUMBER
AD - A109301		
4. TITLE (and Subtitle)		5. TYPE OF REPORT & PERIOD COVERED
ARPA SEMI-ANNUAL TECHNICAL REPORT		Interim 6/1/75 - 11/30/75
		6. PERFORMING ORG. REPORT NUMBER
		LRSM-75-3
7. AUTHOR(s)		8. CONTRACT OR GRANT NUMBER(s)
Heeger, A. J., Director & Principal Investigator		F44620-75-C-0059 ARPA Order 3019
9. PERFORMING ORGANIZATION NAME AND ADDRESS		10. PROGRAM ELEMENT, PROJECT, TASK AREA & WORK UNIT NUMBERS
University of Pennsylvania, Laboratory for Research on the Structure of Matter 3231 Walnut St. /K1, Phila. Pa. 19174		Program 5 D10
11. CONTROLLING OFFICE NAME AND ADDRESS		12. REPORT DATE
Advanced Research Projects Agency 1400 Wilson Boulevard Arlington, Virginia 22209		Dec. 31, 1975
14. MONITORING AGENCY NAME & ADDRESS (if different from Controlling Office)		13. NUMBER OF PAGES
Air Force Office of Scientific Research/NE Building 410 Bolling AFB, D. C. 20332		13
		15. SECURITY CLASS. (of this report)
		U UNCLASSIFIED
		15a. DECLASSIFICATION/DOWNGRADING SCHEDULE
16. DISTRIBUTION STATEMENT (of this Report)		
<p style="text-align: center;">APPROVED FOR PUBLIC RELEASE DISTRIBUTION UNLIMITED</p>		
17. DISTRIBUTION STATEMENT (of the abstract entered in Block 20, if different from Report)		
<p style="text-align: right;">DTIC ELECTE S JAN 6 1982 D</p>		
18. SUPPLEMENTARY NOTES		
19. KEY WORDS (Continue on reverse side if necessary and identify by block number)		
Surfaces and Interfaces; IV-VI Semiconductors; Interface Electromagnetic Modes; Chemisorption; Catalysis; Solid electrode materials; Photoemission; Interfacial kinetics; Intercalated graphite compounds - conductivity; Intercalated graphite compounds - reflectivity; Intercalated graphite compounds - superacids.		
20. ABSTRACT (Continue on reverse side if necessary and identify by block number)		
<p>A summary of the research program funded by ARPA at the University of Pennsylvania Laboratory for Research on the Structure of Matter is presented. The progress and research accomplishments for the period June 1, 1975 to November 30, 1975 are emphasized.</p>		

AD A109301

DTIC FILE COPY

DD FORM 1 JAN 73 1473 EDITION OF 1 NOV 65 IS OBSOLETE

81 12 28 127

SECURITY CLASSIFICATION OF THIS PAGE (When Data Entered)

ARPA Semi-annual Technical Report

6/1/75 to 11/30/75

Accession For	
NTIS GRA&I	<input checked="checked" type="checkbox"/>
DTIC TAB	<input type="checkbox"/>
Unannounced	<input type="checkbox"/>
Justification	
By	
Distribution/	
Availability Codes	
Dist	Avail and/or Special
A	

Sponsored by:  
Advanced Research Projects Agency  
ARPA Order Number: 3019

Contract Number: F44620-75-C-0069

Program Code Number: 5 D10

Principal Investigator:  
Alan J. Heeger  
(215) 243-8571

Name of Contractor:  
University of Pennsylvania-  
Laboratory for Research on  
the Structure of Matter

Project Scientist:  
Alan J. Heeger  
(215) 243-8571

Effective Date of Contract:  
1 June 1975

Short Title of Work:  
Materials Science Research

Expiration Date of Contract:  
30 September 1976

Report No: LRSM 75-3

Amount of Contract: \$355,000

Date of Report: 31 Dec. 1975

Form Approved, Budget Bureau No. 22-R0293

The views and conclusions contained in this document are those of the authors and should not be interpreted as necessarily representing the official policies, either expressed or implied, of the Advanced Research Projects Agency or the U. S. Government.

# 1. Summary of Research Program:

## A. Chemical and Physical Properties of Surfaces and Interfaces - -

The LRSM has a broadly based program of research on chemical and physical phenomena which occur at the surface of materials or at the interface between two materials. The long range goal of this program is to achieve the kind of deep understanding of such phenomena at the microscopic level which we now have about many important phenomena in bulk materials. Over and above the fundamental intellectual interest of the outstanding problems in this area, there are two major reasons for our thrust in this direction. The first is based on new capabilities: New theoretical and experimental techniques have recently been developed or are on the horizon which promise to make possible substantial advances in this field. The second reason is the growing urgency of the need to understand technologically important surface phenomena such as catalysis, which plays a crucial role in the energy and chemical industries, and a variety of surface phenomena which are assuming ever greater importance with the continuing miniaturization of electronic devices.

The primary goal of the Surfaces and Interfaces Program is to develop an understanding, on a microscopic level, of the bonding of and the interaction between adsorbed species on a solid surface. The core of the program is directed specifically to questions concerning the interaction of simple molecules, such as  $H_2$ , CO, and  $C_2$ , with metal atoms of the late transition series when these atoms are in a variety of well-characterized surface environments. Such systems are simple enough to be amenable to experimental and theoretical analysis - both of which are imperative if progress is to be made - and at the same time are of considerable current interest in industrial processes. A variety of experimental and theoretical techniques are being employed by members of the program. One must study experimentally the structure of the bonding surface, the nature of reacting species, bonding configurations of reactants, the kinetics of the formation of surface species, etc. Theoretical effort must focus on the phenomena themselves as well as on the interpretation of experimental techniques and results.

## B. IV-VI Semiconductor Films and Surfaces -

The purpose of this work is to explore and exploit several phenomena in semiconductors, especially lead chalcogenides. Emphasis is placed on possible device applications.

The importance of IV-VI compounds in infrared technology has long been appreciated. Optimum design of devices requires an adequate description

of noise phenomena, which appear to be related to point defects in a complex way. Some of the newer applications of IV-VI devices to pollution monitoring are currently too expensive for large-scale deployment. A need therefore exists for a low-cost, moderate-performance system which may evolve from a combination of thin film growth and integrated circuit technologies.

### ✓ C. Intercalated Graphite Compounds

The research program in the LRSM on intercalated graphite compounds has three ultimate objectives:

- a) to synthesize graphite intercalation compounds with room temperature conductivities comparable to or even greater than that of copper;
- b) to obtain sufficient understanding of the effects of intercalation on the electronic structure to guide the synthesis; and
- c) to develop high-strength composite materials which will allow the practical realization of highly conducting intercalation compounds. ✓

The use of electrical energy in the U. S. is doubling every ten years. This fact, along with the limited supply of fossil fuels, has caused a renewed emphasis on considerations of energy sources and their applications. One aspect being considered is the need for new, inexpensive, efficient electrical conductors. The successful development of an electrical conductor based on graphite intercalated compounds offers the promise of a high efficiency, inexpensive, domestically supplied material.

## 2. Progress and Accomplishments

### A. Chemical and Physical Properties of Surfaces and Interfaces

Plummer and Gustafsson have measured the cross section for photoionizing each valence level of the simple molecules  $N_2$ ,  $O_2$ ,  $CO$ ,  $CO_2$ ,  $N_2O$ ,  $H_2O$ ,  $H_2CO$  and  $CH_4$  as a function of photon energy. These measurements were made in conjunction with theoretical calculations by Davenport and Schrieffer who have extended the scattered wave  $X\alpha$  method of Slater and Johnson to the calculation of photoionized cross sections of diatomic molecules. The method involves a local approximation to the exchange and correlation potential and a spatial average of this potential into the "muffin tin" form. Schroedinger's equation may be solved using an angular momentum expansion. In practice partial waves up to  $l=3$  are required for convergence for photon energies less than 50 eV. Computations are performed in the molecule's rest frame, and then averaged over all orientations to produce

the gas phase cross sections. These show quite good agreement with the measurements of Gustafsson and Plummer for  $N_2$  and CO which were made for photon energies between 18 eV and 40 eV. A particular feature is the prediction of a shape resonance due to the  $l=3$  partial (wave about 10 eV above threshold for the  $4\sigma$  and  $5\sigma$  levels of CO and the  $3\sigma_g$  level of  $N_2$ ). This resonance was shown not to occur for the  $2\sigma_u$  level of  $N_2$ . These predictions are all in excellent agreement with the recent results of Plummer and Gustafsson. The photoemission work appears to be a major breakthrough and has gained wide recognition even prior to publication.

In addition, Davenport and Schrieffer have calculated the differential cross sections for oriented CO and  $N_2$  molecules as a function of angle for several photon energies. These show non-plane wave effects; for example, relatively large cross sections in directions perpendicular to the electric field (this is always zero if a plane wave final state is used). They also show large variations with photon energy and polarization of the incident light. For molecular orbitals of adsorbates which are relatively unaffected by bonding to the substrate we expect the photoionization cross section to be determined largely by the molecular potential rather than the underlying solid. For these, the angular distribution of the photoelectrons could be used in conjunction with these calculations to deduce the molecule's orientation relative to the surface.

An improved multiple-scattering  $X\alpha$  (MSX $\alpha$ ) method was applied by Schrieffer and Danese to the calculation of the potential surface of the NiCO molecule. This improved MSX $\alpha$  method includes the corrections to the total energy and eigenvalues which result from non spherical and non constant components in the electron density and has been shown to be a reliable method for the calculation of potential surfaces for diatomics. The principal conclusion from these essentially completed calculations is that the CO bond when CO bonds to a nickel atom is lengthened and weakened. To determine whether this is a feature of CO adsorption on a nickel surface future calculations on the clusters  $Ni_2CO$  and  $Ni_4CO$  are needed. If this behavior should prove to be a common feature of these three systems then it could be concluded that this same feature is characteristic of CO on nickel. With this conclusion a major step in explaining the unique properties of CO on nickel will have been made. It should be noted that these are pioneering calculations not previously feasible and not previously attempted by any other method with any hope of success.

Prof. Burstein and collaborators have studied the interface EM modes of a surface quantized plasma layer at a semiconductor surface. The theory includes the interaction of the interface EM waves with the inter-subband excitations of the surface quantized levels, and uses a model in which the plasma layer is represented by an anisotropic plasma slab having

an effective thickness  $d^*$  and a spatially uniform effective dielectric tensor whose principal components are given by

$$\begin{aligned}\epsilon_x(\omega) &= \epsilon_{\infty x} \left( 1 - \frac{4\pi \bar{n}_s e^2}{\epsilon_{\infty x} m_x d^* \omega(\omega + i\gamma_x)} \right) \\ \epsilon_z(\omega) &= \epsilon_{\infty z} + \sum_{ij} \frac{4\pi \bar{n}_s e^2 f_{ij}}{m_{ij} d^* (\omega_{ij}^2 - \omega^2 - i\gamma_{ij} \omega)} \\ \epsilon_y(\omega) &= \epsilon_x(\omega)\end{aligned}\quad (1)$$

where  $x, y, z$  are the direction of propagation of the modes, the normal to the sagittal plane and the normal to the slab respectively;  $\gamma_x$  is the damping constant of the carriers for motion in the  $x$  direction;  $\bar{n}_s$  is the effective surface charge density;  $\omega_{ij}, f_{ij}, \gamma_{ij}$  are the frequency, oscillator strength and damping constant of the  $i$ - $j$  inter-subband electronic excitations.

The interface EM modes of the anisotropic plasma slab include bound EM modes, i. e., surface EM waves and guided modes, and virtual modes, i. e., leaky surface EM waves and leaky radiative guided modes, which occur in different frequency-wave vector regions.

In the absence of inter-subband excitations, the "bound" modes of the asymmetrical  $\text{SiO}_2$ -anisotropic plasma-Si slab configuration are wave-guide modes. The dispersion curve of the  $m = 0$  wave-guide modes, at small values of the propagation wave vector  $k_{||} = k_x$ , such that  $2\pi k_{za} d^* \ll 1$ , is identical to that for the "surface" modes of the 2-d (zero thickness) electron gas model.

When one includes the interaction of the interface EM modes with the inter-subband excitations and, for simplicity, only takes into consideration the inter-subband excitation,  $\omega_{01}$ , from the ground state to the next higher subband, one finds that the  $m = 0$  wave guide modes are not photon-driven type interface EM waves at  $0 < \omega < \omega_{01}$ , and regular interface EM waves at  $\omega_{01} < \omega < \omega_{01}^*$ , but remain wave-guide modes at  $\omega > \omega_{01}^*$ , where  $\omega_{01}$  and  $\omega_{01}^*$  are the frequency at which  $\epsilon_{za}(\omega)$  is a pole and a zero respectively. In addition, the leaky EM modes bend toward large value of  $k_{||}$  in the region  $\omega_{01} < \omega < \omega_{01}^*$ , where both  $\epsilon_{za}$  and  $\epsilon_{xa}$  are negative and turn into regular surface EM waves when  $k_{||}$  becomes larger than  $\epsilon_c^{\frac{1}{2}} \frac{\omega}{c}$ . Virtual (radiative) modes, which correspond to Berreman-type slab modes, appear at  $\omega > \omega_{01}^*$ .

The "bound" modes can only be coupled to TM volume EM waves by augmenting the wave vector of the volume waves incident on either the Si or the  $\text{SiO}_2$  side. The virtual modes on the other hand can be coupled to TM volume EM waves by using Si as its own "ATR" prism.

The calculated ATR spectrum of the Si-anisotropic plasma- $\text{SiO}_2$  configuration, for the case where the Si is used as its own prism, exhibits some interesting features. (i) At incident angles  $A$  in the Si prism, larger than  $A_{c1}$  the critical angle for the Si- $\text{SiO}_2$  interface, where  $\sin A_{c1} = (\epsilon_{xb}/\epsilon_{xc})^{1/2}$ , the reflectivity as a function of frequency, shows dips at  $\omega_1 \approx \omega_{o1}^*$  (instead of at  $\omega \approx \omega_{o1}$ ) and at  $\omega \approx \omega_2$ , where  $\omega_2$  satisfies  $\sin \theta_{c2} = (\epsilon_{xa}(\omega_2)/\epsilon_{xc})^{1/2}$ , and  $\theta_{c2}$  is the critical angle for the Si-anisotropic plasma interface. The dip at  $\omega_1 \approx \omega_{o1}^*$  corresponds to the coupling of the incident TM waves with the leaky surface EM waves. The dip at  $\omega_2$  is related to the excitation of Berreman-type modes.

It should be emphasized that the model used is a zeroth order approximation, in which all of the  $z$  dependent quantities, such as the charge density, the dielectric constants, etc., are replaced by their average values as spatially uniform parameters. A more realistic model, which takes into account the actual wave functions of the electrons in the space charge region, is under investigation.

Experimentally Burstein and associates have used surface EM waves generated by prism coupling at an Ag-air interface as excitation source to observe a marked enhancement of the fluorescence intensity of very thin layers of rhodamine 6G over that obtained by volume EM wave excitation. The enhancement of the fluorescence intensity is a direct manifestation of the enhanced electric fields that occur when surface EM waves are generated at metal-air interfaces. A similar enhancement may be expected in the intensity of Raman scattering by overlayers of molecules on metal surfaces. These enhanced fields can be used to enhance Raman scattering as well as fluorescence by overlayers on metals.

Wayland and associates have continued to evaluate the nature of chemisorption of small molecules by metallo-sites, and develop models for the binding and modified chemical behavior of molecules at surfaces. Transition and rare earth metal chelate complexes can function as chemisorption materials. Recent efforts have been focused on the chemisorption of  $\text{O}_2$ ,  $\text{SO}_2$ ,  $\text{CO}$ ,  $\text{NO}$ ,  $\text{N}_2\text{O}$  and  $\text{H}_2\text{O}$  by planar four coordinate metal chelate species. These materials have open coordination sites, which bind the donor or acceptor molecule.

One specific set of materials currently being evaluated are the metallo porphyrins. Coordination of a porphyrin ligand with a metal(II) ion imposes a local square planar donor site distribution around the metal ion

and provides a series of weak chemisorption materials that change principally in the number of d valence electrons associated with the central metal ion. Low spin planar cobalt(II) chelates ( $d^7$  metal ion) have a single unpaired electron in the  $d_{z^2}$  molecular orbital, which has a large probability normal to the molecular plane. Cobalt(II) tetraphenylporphyrin reversibly adsorbs  $O_2$ ,  $SO_2$ , CO, NO and many neutral donors. One molecule of either  $O_2$ , CO or  $SO_2$  is found to bind at each metal site. Molecular oxygen is found to function as an electron acceptor in this system, reversibly forming coordinated  $O_2^-$  species. Magnetic resonance studies show that  $SO_2$  and CO function predominately as donors with the odd electron largely retained in the metal based orbitals. The reversible adsorption of  $SO_2$ , CO, and  $O_2$  by Co(II) chelates gives them potential in gas separations and in catalytic applications, such as the oxidations of CO and  $SO_2$  and  $CO_2$  and  $SO_3$ . Nitric oxide reacts reversibly with the Co(II) macrocycle to form complexes involving 1-3 NO molecules. One of these species involves monodentate coordinated  $N_2O_2^{-2}$  which has potential in the catalytic reaction of CO and NO to form  $CO_2$  and  $N_2O$  or  $N_2$ .

The Fe(II) macrocycles adsorb one and two molecules of CO and NO and mixed species. Thermodynamic and spectroscopic characterization of these diatomic molecule species are in progress. Electron transfer between two adsorbed NO molecules produces  $NO^+$  and  $NO^-$  sites. Similarly the Mn(II) macrocycles adsorb one or two NO molecules per metal center.

A systematic model for anticipating the general structural and electronic features of chemisorbed diatomic molecules has been proposed and studies on new materials of this type are being used in assessing the range of applicability for this model.

We are continuing our attempt (Caspari) to study hyperfine interactions and in particular, quadrupole interactions in atoms adsorbed on clean single crystal metallic surfaces as a function of coverage and substrate temperature in order to obtain information regarding the electron densities and electric field gradients in the immediate vicinity of the adatoms and to determine the symmetry of the adsorption sites. In addition, this study should yield valuable information regarding surface diffusion on a macroscopic scale, clustering and island formation.

The method used is that of perturbed integral and time differential  $\gamma$ - $\gamma$  angular correlations. This technique is a suitable tool for these experiments since it requires few atoms and is carried out on labelled radioactive isotopes deposited on the surface so that one can be sure that the measurements reflect the conditions on the surface rather than the bulk.

These experiments form part of a coordinated program carried out at the University of Pennsylvania's LRSM designed to obtain information



regarding the geometric location of single adatoms on a surface and on the structural dependence of surface interactions. Such knowledge is vital in the development of a microscopic model of chemisorption. In addition to the hyperfine interaction measurements this problem is being studied by field ion microscopy (W. Graham) and angular resolved photoemission and Auger spectroscopy (Plummer and Gustafsson). The experiments are coordinated by a theoretical program (Schrieffer and Soven) designed to evaluate and interpret the complementary experiments.

The model system we have chosen for this study are adsorption of cadmium and hafnium atoms on tungsten and nickel, since all three types of measurements can be conveniently carried out with Cd and Hf atoms. Tungsten was chosen because much experimental data on chemisorption has been collected on tungsten surfaces while nickel is more amenable to theoretical analysis.

In addition we plan to study the problem of catalysis directly by determining the change in the wavefunctions of the surface layer of the substrate due to the presence of adsorbed gases such as  $H_2$ ,  $CO$ ,  $CO_2$ ,  $O_2$ ,  $CH_4$ , etc. using a monomolecular layer of radioactive isotopes on the crystal surface.

In the battery related work, Worrell and associates have prepared new solid electrode materials which look particularly promising by intercalating  $2H-TaS_2$  with lithium and sodium. Intercalation is achieved with organic solutions containing the appropriate alkali metal as an ion (n-butyllithium) and sodium naphthalide in tetrahydrofuran (THF). It was found that intercalation was practically complete in 2-3 days.

These electrode materials give unusually high open circuit voltages with reference to the pure metal at ambient temperatures. For example, the cell  $Li | Li^+ (\text{propylene carbonate}) | Li_{0.83}TaS_2$  gives a stable open circuit voltage of 1.67 volts at room temperature. Another cell  $Na | Na - 8Al_2O_3 | Na_{0.83}TaS_2$  has an open circuit voltage of 1.00 volts at  $200^\circ C$ .

These results are especially encouraging since electrodes with less than 80% lithium or sodium are expected to yield even higher voltages. For example the sodium cell above has a voltage of 1.5 volts when the electrode is  $Na_{0.68}TaS_2$ .

Belton's studies of interfacial kinetics are directed toward an understanding of the factors which influence the rates of reaction of gases with liquid and solid metals and are of importance in controlling treatments such as nitridation and carburization and in the understanding and control of

refining processes. The marked effects on interfacial reaction rates of the strongly surface active elements need to be quantitatively understood.

Laboratory experiments on the rates of dissociation of, particularly,  $\text{CO}_2$  are being carried out on several metals. Literature work is mainly in the area of reinterpretation of the available surface tension data for Group VI solutes and the application of the results to existing interfacial kinetic studies.

It has been found that the considerable body of information on the depression of the surface tension of liquid iron by Group IV solutes, due mainly to Kozakevitch and his co-workers (Mem. Sci. Rev. Met., 1961, vol. 58, pp. 401-13, pp. 517-34, pp. 932-47) is consistent with an ideal site fillage isotherm of the form

$$\sigma^P - \sigma = RT\Gamma_i^0 \ln(1 + Ka_i)$$

where  $\sigma^P - \sigma$  is the depression of the surface tension of the pure liquid metal,  $\Gamma_i^0$  is the saturation coverage by the solute,  $a_i$  is the bulk thermodynamic activity of the solute, and  $K$  is a coverage independent, temperature dependent adsorption coefficient. Other work on sulfur in copper and oxygen in silver is also closely described.

These thermodynamic adsorption coefficients have been found to be remarkably good in quantitatively describing the poisoning effects of these solutes on several interfacial reactions. In particular, the widely differing effects of oxygen (Pehlke and Elliott: Trans. AIME, 1963, vol. 227, pp. 844-55) and tellurium (Mowers and Pehlke: Met. Trans., 1970, vol. 1, pp. 51-56) on the rate of absorption of nitrogen into liquid iron have been found to be in close accord with the surface coverages of these elements from the above surface tension isotherm.

The kinetics of decarburization of liquid iron have been studied between 1160 and 1600°C under conditions where mass transport of reactants is not rate determining. Studies with continuously carbon-saturated iron and with iron with varying carbon concentrations have been used to show that the slow step at high concentrations of carbon is independent of carbon concentration and is first order with respect to the pressure of  $\text{CO}_2$ . For high purity iron, the forward rate constant, in  $\text{mole cm}^{-2} \text{ sec}^{-1} \text{ atm}^{-1}$ , is given by the equation

$$\ln k_f = -11700/T - 0.48$$

The results appear to be consistent with the chemisorption process as the rate limiting step. Sulfur, antimony, and tin have been found to slow down this reaction and, particularly in the case of sulfur, the interference is in

good accord with Langmuir adsorption of the element. A residual rate on the fully covered sulfur surface has been found, the activation energy for this residual rate being very close to that for the dissociation of  $\text{CO}_2$  on the pure iron surface.

#### B. IV-VI Semiconductor Films and Surfaces

The energy band structure of the high pressure (NaCl) phase of CdS has been calculated (Rabii) using a fully relativistic symmetrized augmented-plane-wave method. The results have been used to obtain density-of-state histograms over a 30 eV range. Our calculations indicate that CdS in this phase is an indirect semiconductor with a forbidden-gap of 1.5 eV, which is in agreement with the experimental data. The valence band has two nearly degenerate maxima at L and at  $\pi/a$  (110) in the  $\Sigma$  directions. The conduction band similarly has one minimum at  $\Gamma$  and another set at X at almost the same energy.

Optical absorption and thermoreflectance spectra were reported by Fischer for the  $E_1$ ,  $E_1 + \Delta_1$  doublet in  $\text{Pb}_x\text{Cd}_{1-x}\text{S}$  metastable epitaxial films (NaCl structure). The bowing parameter for  $E_1$  is  $\sim 1$  eV or less, while for  $E_1 + \Delta_1$  we find 4.1 - 4.5 eV. The latter is much larger than any value reported heretofore, and may be explained by the large fluctuation potential arising from atoms of different valence randomly occupying the metal sublattice. Differences between  $E_1$  and  $E_1 + \Delta_1$  imply strong disorder-induced mixing of states which is concentration-dependent.

Matrix isolation studies (Nixon) of IV-VI compounds and related systems has continued. Condensing onto a cold finger (4K-10K) atoms or molecules from the vapor state together with a large amount of an inert gas such as argon, and thereby trapping the atoms or molecules in the solid inert gas matrix is a convenient technique for preserving and studying the spectral properties of such species. We have continued experiments to define the role the matrix itself plays in the spectral properties of the impurity molecules. These studies have involved primarily absorption spectroscopy and laser-induced luminescence.

The role of the matrix in assisting photon absorption and in the relaxations processes of the excited molecules has allowed us to continue to observe hitherto unreported electronic states of a variety of molecules ( $\text{GeS}$ ,  $\text{Pb}_2$ ,  $\text{Bi}_2$ ,  $\text{PbBi}$ ,  $\text{Se}_2$ , etc.). We have also observed new cases in which visible laser light produces by biphotonic processes significant light emission in the ultraviolet.

Matrices deposited at 10K can be "annealed" by raising the temperature slightly for a while and in many cases of annealed matrices, most of the light intensity in both absorption and emission is contained in sharp

"zero-phonon" vibronic bands of the electronic-vibrational band system of the impurity molecule. In such cases, isotopic band structure can often easily be resolved. With our tunable laser source we have selectively caused absorption and emission by a single chosen isotopic variant of the molecule. For example in PbS, molecules containing  $^{34}\text{S}$  have been selectively excited.

We have observed in emission some of the electronic states of the tetratomic species  $\text{Pb}_2\text{S}_2$  and  $\text{Pb}_2\text{Se}_2$ .

The matrix isolation technique has been used as an analytical tool to characterize the species,  $\text{S}_2\text{N}_2$ ,  $\text{S}_4\text{N}_4$  and others, which evolve in the volatilization of polymeric sulfur nitride.

### C. Intercalated Graphite Compounds (Fischer, Thompson, Vogel, Girifalco)

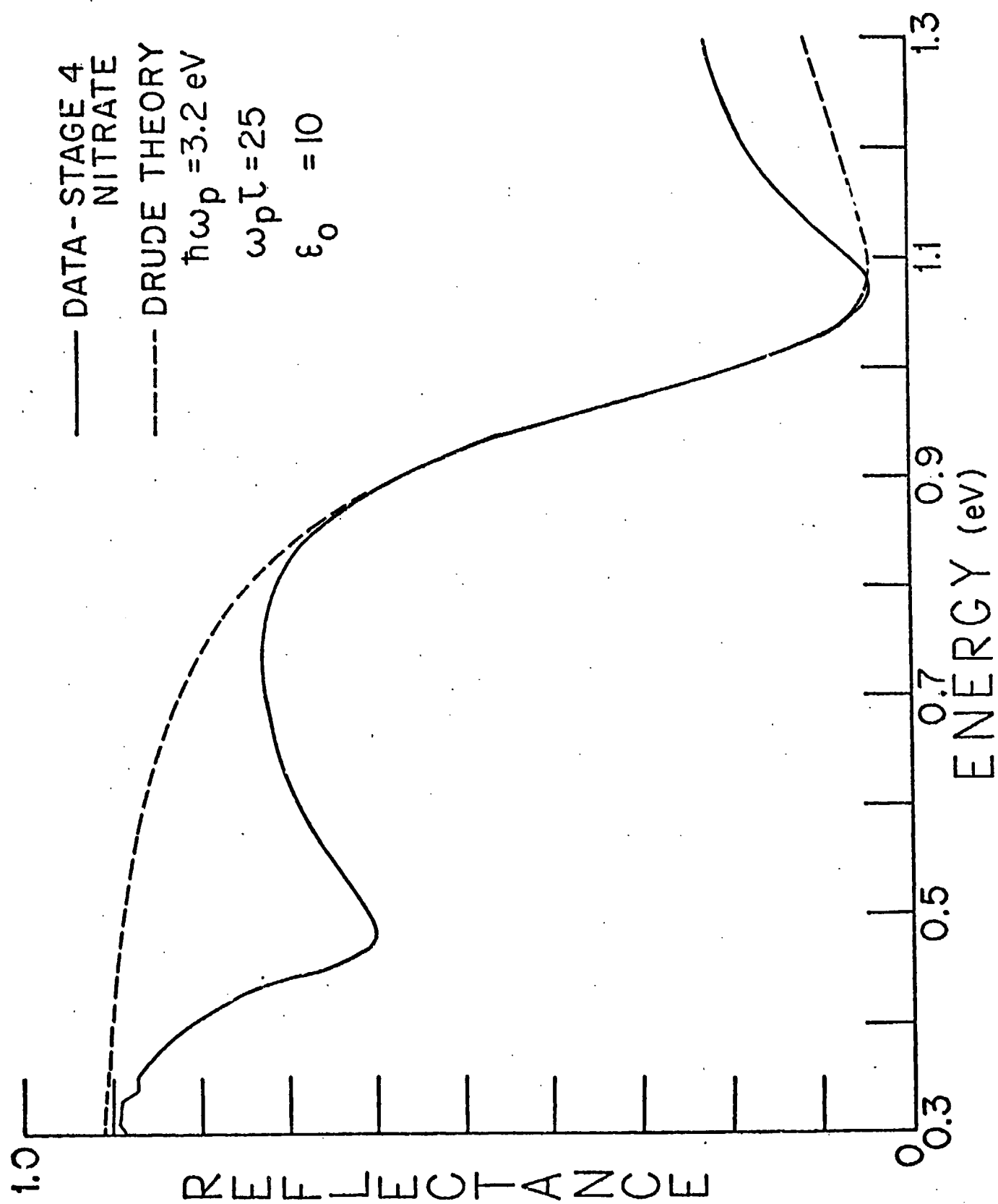
Commercial graphite powder (spectrographic grade, 10-40 micron particle size) was intercalated with  $\text{SbF}_5$  liquid in a sealed copper tube. After intercalation the tube was swaged in several passes, increasing the density of graphite to 85% of the theoretical value. The room temperature dc conductivity of the compacted core was  $8 \times 10^6 (\Omega \text{ cm})^{-1}$ , about 30% higher than that of OFHC copper. The terminal resistance of the composite has remained stable for 3 months.

This preliminary result has 3 important implications:

1. Conductivity appears to increase with acid strength (although the detailed physics are still unknown), which suggests even higher conductivities are possible.
2. Swaged powder composites provide an alternative to fibers for practical application of intercalated graphite.
3. Swaging in a sealed tube appears to overcome the notorious instability of strong acid intercalates.

Optical reflectance studies have revealed plasma edge phenomena characteristic of metallic behavior for various intercalated graphite compounds. The plasma frequency depends in detail on the intercalate; such studies therefore provide fundamental information on the charge transfer and scattering mechanisms.

Drude-type fits have been obtained for the near IR-visible reflectance spectra of several compounds. Typical data are shown in Fig. 1. The fit



in the edge region (0.8-1.1 eV) is excellent. The rise in R signifies interband effects not included in the theory. Most remarkable is the strong dip at  $\sim 0.5$  eV. This minimum varies greatly in amplitude and somewhat in position from sample to sample. Its origin is the subject of continuing study.

Drude parameters are assembled in Table 1. The progression of  $\hbar\omega_p$  to higher values as the acid strength increases could be due either to greater fractional ionization per inserted molecule or to a larger density of inserted molecules. Both effects play a role; detailed chemical analysis is in progress to sort out the two effects.

Scaling the plasma frequencies as measured with the known  $\sigma$  of  $\text{HNO}_3$ -graphite suggests  $\sigma \sim 1.5 \sigma$  (copper) for the superacid compound ( $\text{SbF}_5 + \text{HF}$ ). However, the optical conductivity  $\sigma_{\text{opt}} = \omega_p^2 \tau / 4\pi$  is always a factor of 40-100 less than  $\sigma_{\text{dc}}$  in cases where both have been measured. This surprising result requires further study.

A theoretical study of intercalated compounds has been initiated. Ordered interstitial compounds with metallic properties can in principle be synthesized from isotropic (3-D), layer-type (2-D) or linear (1-D) host crystals. Charge transfer between interstitial atoms and host lattice generally increases the free carrier density and the phonon-free carrier scattering rate. A simple calculation suggests that the conductivity increases most rapidly with interstitial concentration in the 1-D case, least rapidly in 3-D. Data for intercalated graphite do not generally fit the predictions of the model except in cases where the interplanar spacing is anomalously large (10Å or greater).

TABLE 1

Material	Comments		C-I-C Distance Å	$\hbar\omega_p$ (eV)	$\tau$ (sec.)
$\text{HNO}_3$ Stage 4	air-exposed		7.75	3.2	$3 \times 10^{-15}$
$\text{SbF}_5$	air-exposed		8.41	3.5	$3 \times 10^{-15}$
$\text{SbF}_5 + \text{HF}$ Stage 1	air-exposed		8.38	4.0	$6 \times 10^{-15}$
	N <sub>2</sub> gas ambient	center of bar		4.7	$3 \times 10^{-15}$
		just below surface		4.9	$3 \times 10^{-15}$
		original surface		6	-